NSF/DOE Thermoelectrics Partnership: Purdue – GM Partnership on Thermoelectrics for Automotive Waste Heat Recovery

PI: Xianfan Xu, xxu@purdue.edu
co-PIs: Timothy S. Fisher, Stephen D. Heister, Timothy D. Sands, Yue Wu

In collaboration with Gregory Meister, James Salvador of General Motor Global R&D

Scope

Targeted areas:

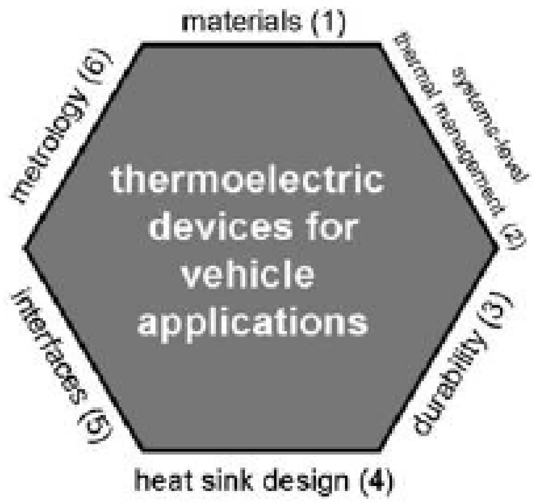

(1) Investigating skutterudites (currently used as the TE material at GM) using ultrafast time-resolved vibration spectroscopy,
(2) Developing nanowire thermoelectric materials,
(3) Developing metal-semiconductor superlattice laminates ,
(4) Developing efficient heat exchanger and system level thermal design,
(5) Developing CNT thermal interface materials.

Investigation of Resonant Vibrations in Filled Skutterudites

- Thermal conductivity reduction in skutterudite via filling that scatters phonons
- Ultrafast dynamics studies to improve the understanding of the filled elements in skutterudites for phonons scattering and thermal conductivity reduction

Mitsch metal		Single and triple elements	
Composition	**Representation**	**Composition**	**Representation**
$Co_{0.9}Fe_{0.1}Sb_3$	$Co_{0.9}$/M2604	$Ba_{0.26}Co_4Sb_{12.01}$	M3402
$Mm_{0.55}Fe_{2.44}Co_{1.56}Sb_{11.96}$	$Mm_{0.55}$	$Yb_{0.21}Co_4Sb_{11.92}$	M3403
$Mm_{0.65}Fe_{2.92}Co_{1.08}Sb_{11.98}$	$Mm_{0.65}$	$La_{0.14}Co_4Sb_{11.99}$	M3404
$Mm_{0.72}Fe_{3.43}Co_{0.57}Sb_{11.97}$	$Mm_{0.72}$	$Yb_{0.05}La_{0.05}Ba_{0.08}Co_4Sb_{11.92}$	M3405
$Mm_{0.82}Fe_4Sb_{11.96}$	$Mm_{0.82}$		

Ultrafast Time-resolved Measurement

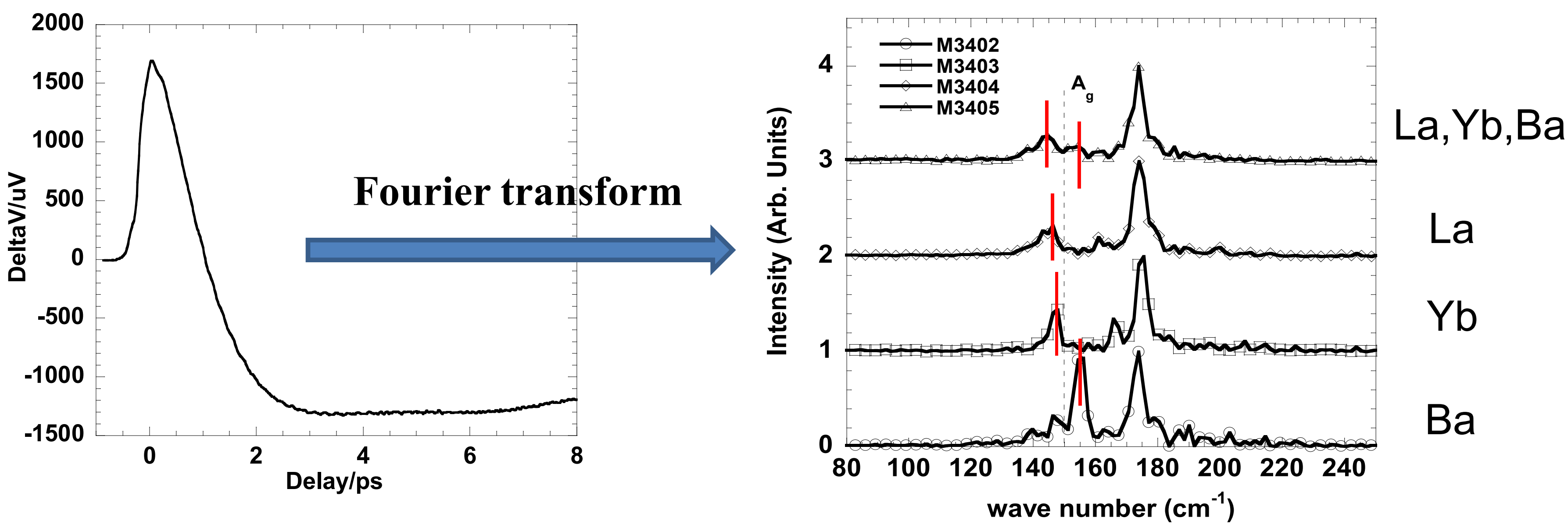

- The mode(s) around 150 cm^{-1} are caused by (strong) interactions between the filled elements and the skutterudite cages. These modes are not observed in the unfilled samples.
- The mode around 175 cm^{-1} has its counterpart in the Raman spectrum. The Raman active modes involve no filling atom motion
- Two modes near the low energy A_g mode are observed in the triple-filled samples caused by different filling atoms.

Lattice Thermal Conductivity

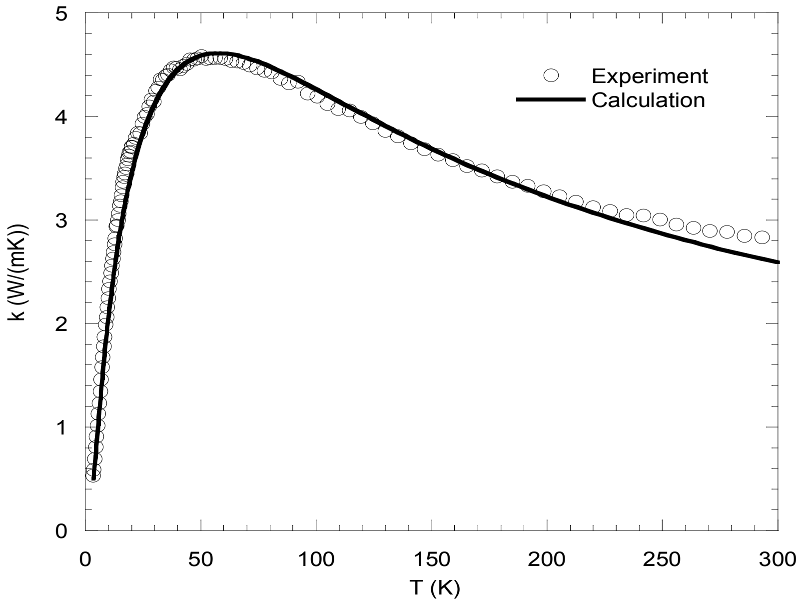

$$\kappa_L = \frac{k_B}{2\pi^2 v}\left(\frac{k_B T}{\hbar}\right)^3 \int_0^{\theta_D/T} \frac{x^4 e^x}{\tau_C^{-1}(e^x - 1)^2} dx,$$

$$\tau_C^{-1} = \frac{v}{L} + A\omega^4 + B\omega^2 T \exp\left(-\frac{\theta_D}{3T}\right) + \boxed{\frac{C\omega^2}{(\Omega^2 - \omega^2)^2}}$$

The resonant frequencies Ω are obtained from the ultrafast time-resolved measurements.

Sample	L (um)	A (10^{-43} s^3)	B (10^{-18} sK^{-1})	C1 (10^{37} s^{-3})	C2 (10^{37} s^{-3})
$Co_{0.9}$/M2604	2.48	79.44	5.84	0	0
M3402	2.87	144.86	3.97	1.11	0
M3403	6.83	214.95	3.04	10.62	0
M3404	5.74	112.15	4.21	11.50	0
M3405	3.71	186.92	4.67	6.64	2.31

Topological Studies of Heat Exchange in TEG

- Objective:
  - Optimize heat exchanger topology and arrangement of Thermoelectric Modules (TEM) in a Thermoelectric Generator (TEG)
  - Maintain exhaust pressure drops within permissible limits
- Methodology:
  - Skutterudites (S) , Bismuth Telluride (B) and hybrid (SB) arrangements were considered to maximize power generation
  - Heat transfer model combined with TEM performance to optimize TEG configuration for fixed volume and/or number of TEMs

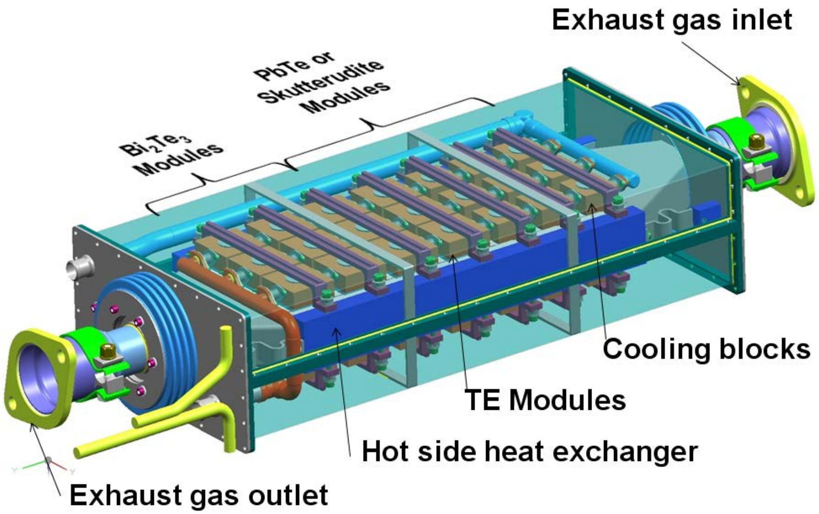

Longitudinal Flow Configuration

- High aspect ratio configuration similar to current TEG systems with TEM blocks arranged on top and bottom surfaces
- Plate fin type heat exchanger integrated inside box
- GM baseline geometry for exhaust gas mass flow rates between 20 and 100 g/s at 550°C
- TEGs using Skutterudites (S) and hybrid (SB)

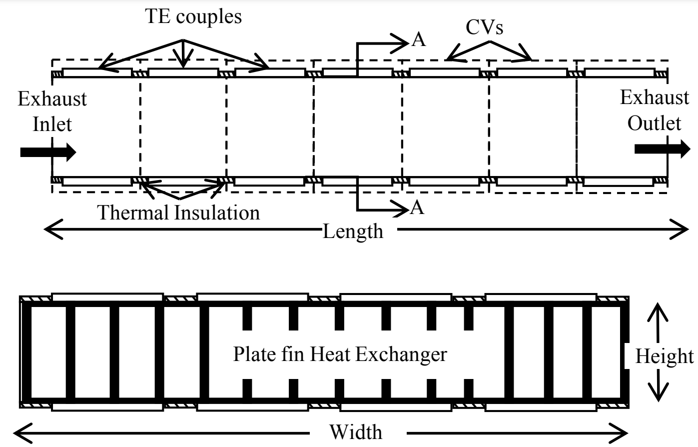

Schematic of TEG (top) and AA cross-sectional view (bottom)

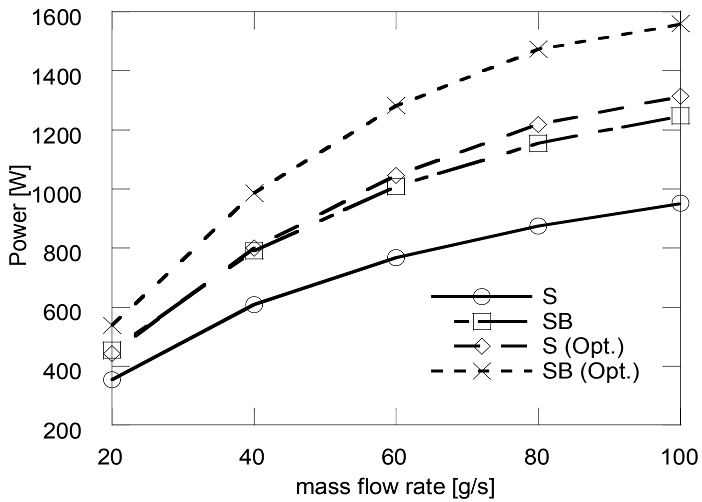

Power output vs. Mass flow rate. (1) Hybrid performs better than using skutterudite alone, (2) optimizing fin dimension is important

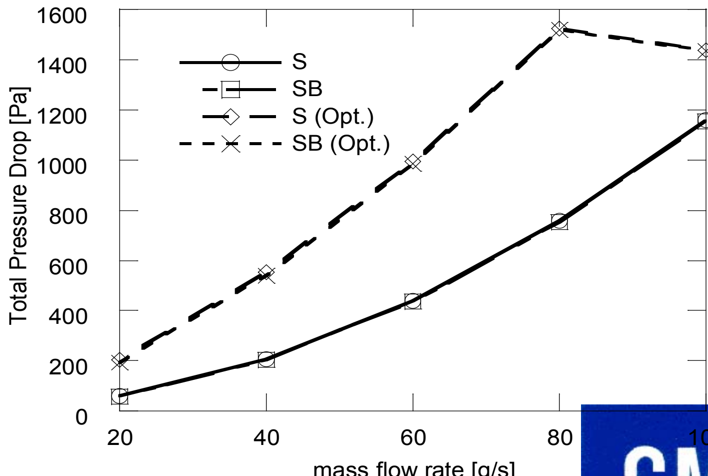

Pressure drop vs. mass flow rate

Longitudinal Flow Configuration

- TEG geometry optimized by varying dimensions and keeping the volume constant (S only)
- Increasing aspect ratio (width/length) increases power output and decreases pressure drop

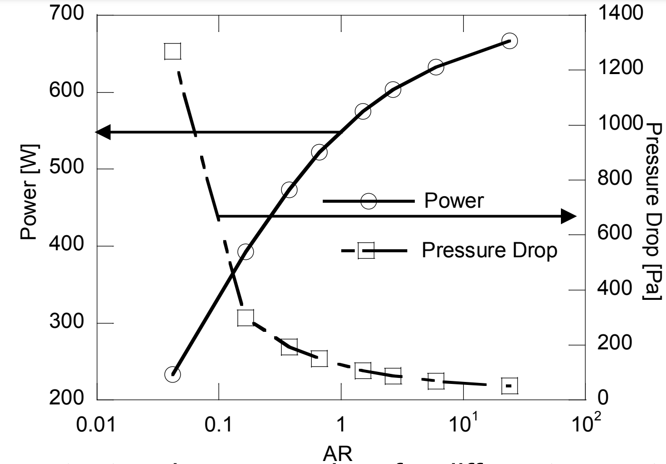

Power output and pressure drop for different aspect ratios (w/l) for 48 skutterudite modules at mass flow rate of 35 g/s

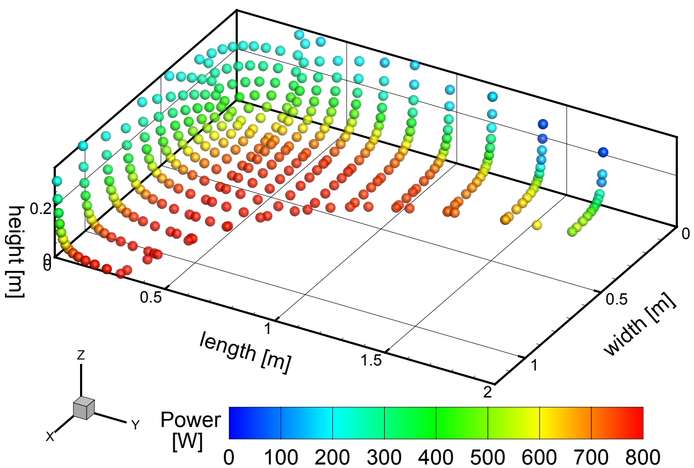

3D contour plot for TEGs at optimized fin configurations at a flow rate of 35 g/s

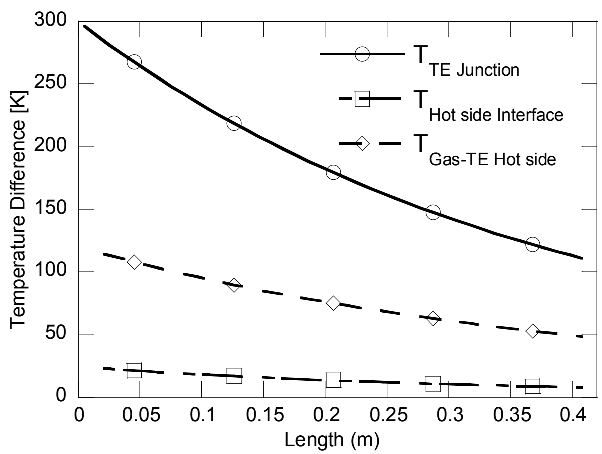

Temperature differences across materials along flow direction

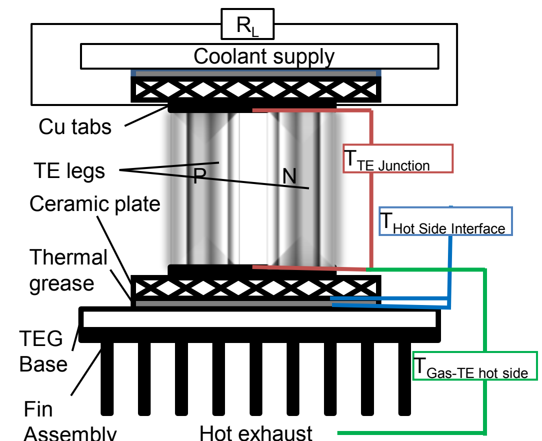

Transverse Flow Configuration

- Exhaust flow distributed axially from centrally-located inlet pipe – gas flows in transverse direction
- TEMs placed on opposing sides of plates integrated vertically inside the box volume
- Separate channels for hot gas flow (red) and coolant flow (blue)
- Plot represents power output for a TEG height equal to one skutterudite TEM width (5.08 cm) for varying aspect ratio (width/length)

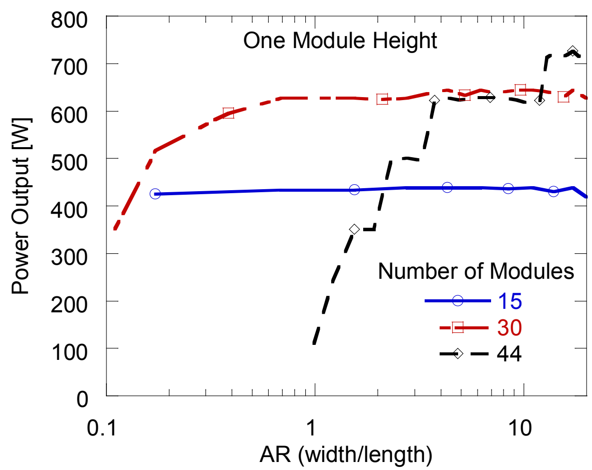

Power output variation with aspect ratio (width/length) for different number of modules

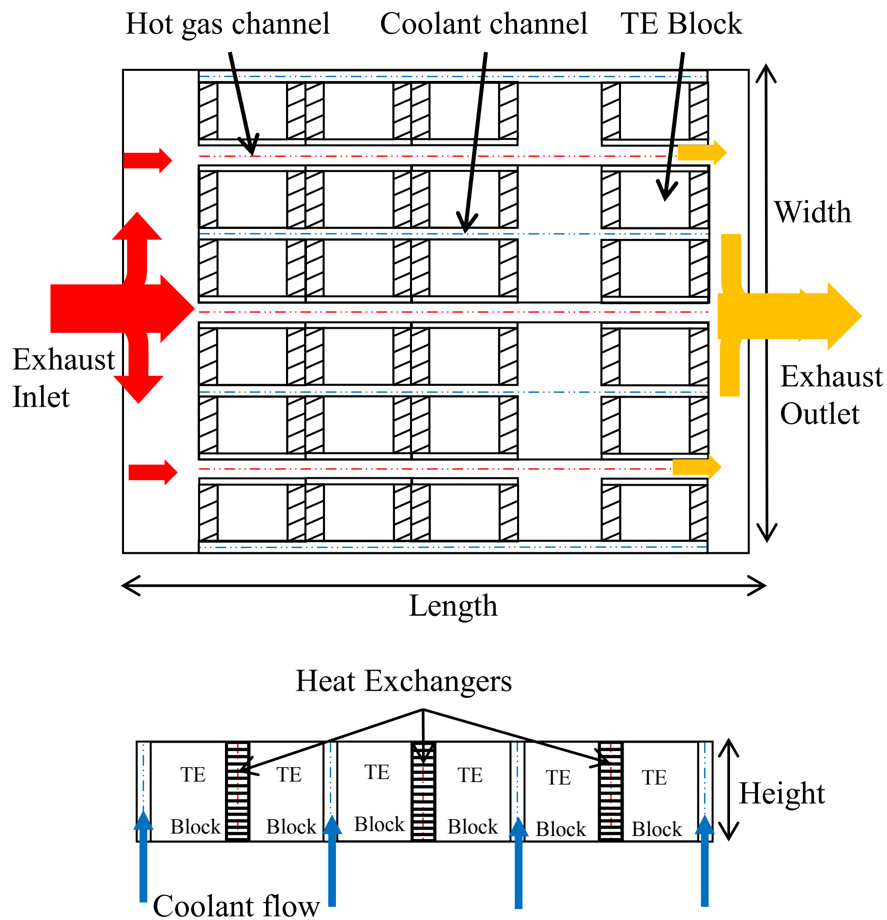

Top view of TEG (top) and front view (bottom)

Transverse Flow Configurations

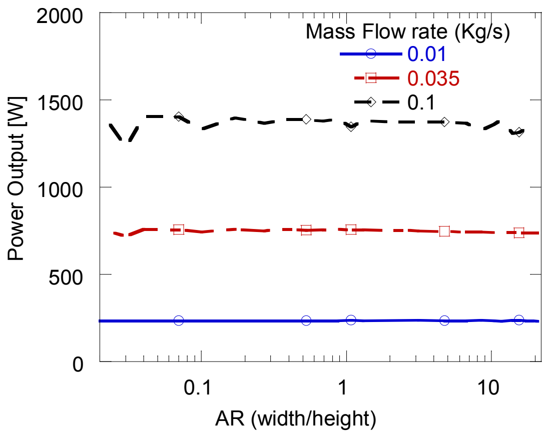

Power output at varying ARs (width/height) for a range of mass flow rates

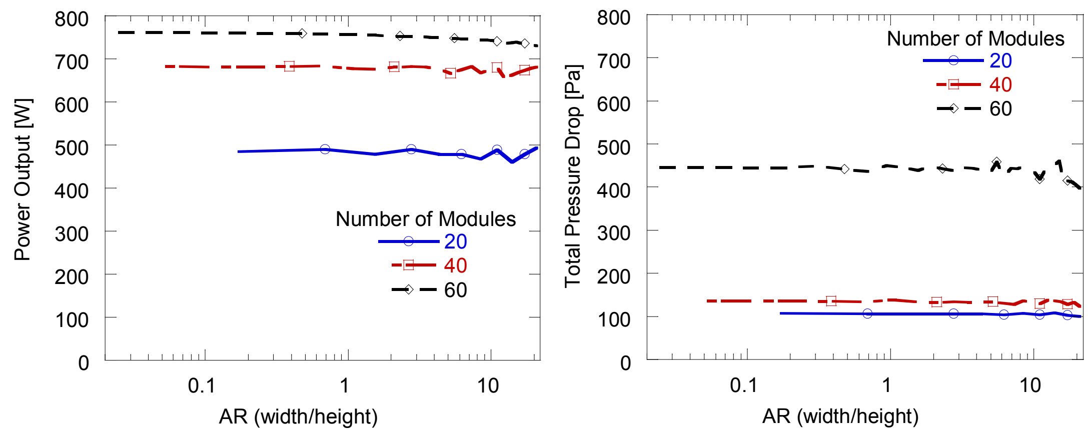

Power output (left) at varying ARs for different number of skutterudite modules and corresponding pressure drop (right)

Transverse flow configuration is superior as more TEMs operate near optimal ZT temperature

- less TEMs needed
- Less pressure drop

The method can be extended to other geometries

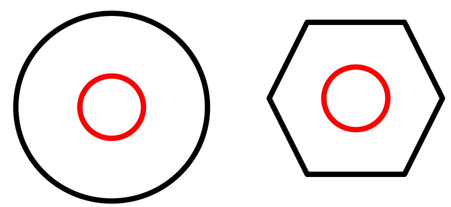

Circular symmetric geometries

Carbon Nanotubes Interfaces for TEGs

- Insertable films with CNT arrays have the potential to reduce the thermal interface resistance between the TE module and the heat source or cold sink, leading to a significant increase in TE efficiency.
- CNT arrays are synthesized on a substrate material using microwave plasma chemical vapor deposition.
- In use, the CNT arrays increase the contact area with the opposing material, leading to a decreased thermal resistance at the interface.

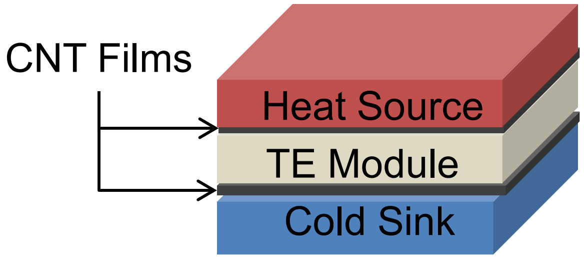

TE System Configuration

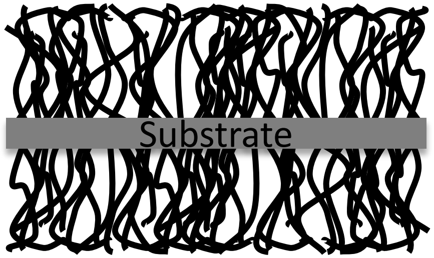

CNT Film – Substrate with CNT Arrays

Enhancement of TE Interfaces with CNT Arrays

- CNT arrays have successfully been synthesized on three candidate substrate materials: copper foil, graphitic foil, and alumina.

- Copper foil coated on both sides with CNT arrays - The thermoelectric power generation is increased by 20% compared with standard thermal interface materials.

CNT Arrays on Cu Foil

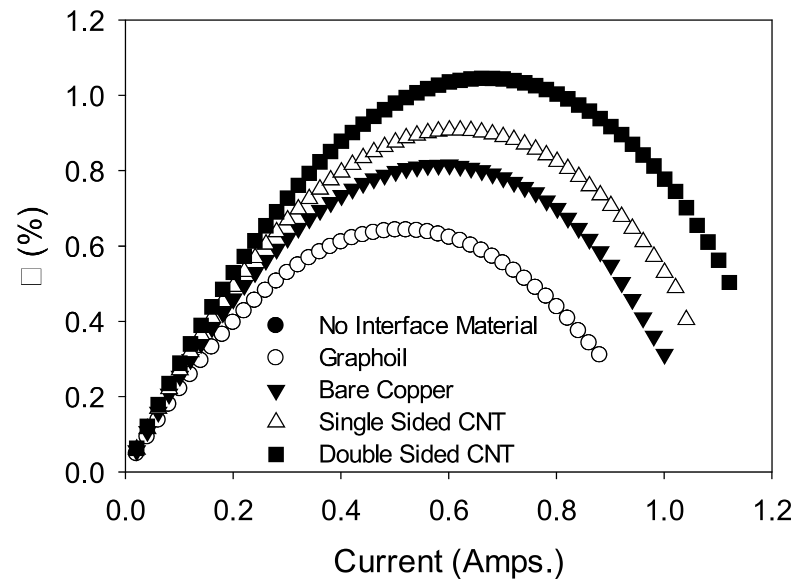

TE Efficiency vs. Current with Various Interface Materials.
Single Sided CNT and Double Sided CNT refer to arrays on Cu foil

PURDUE UNIVERSITY

GM

Nanostructured Thermoelectric Materials

- n-type Bi_2Te_3 Nanowires

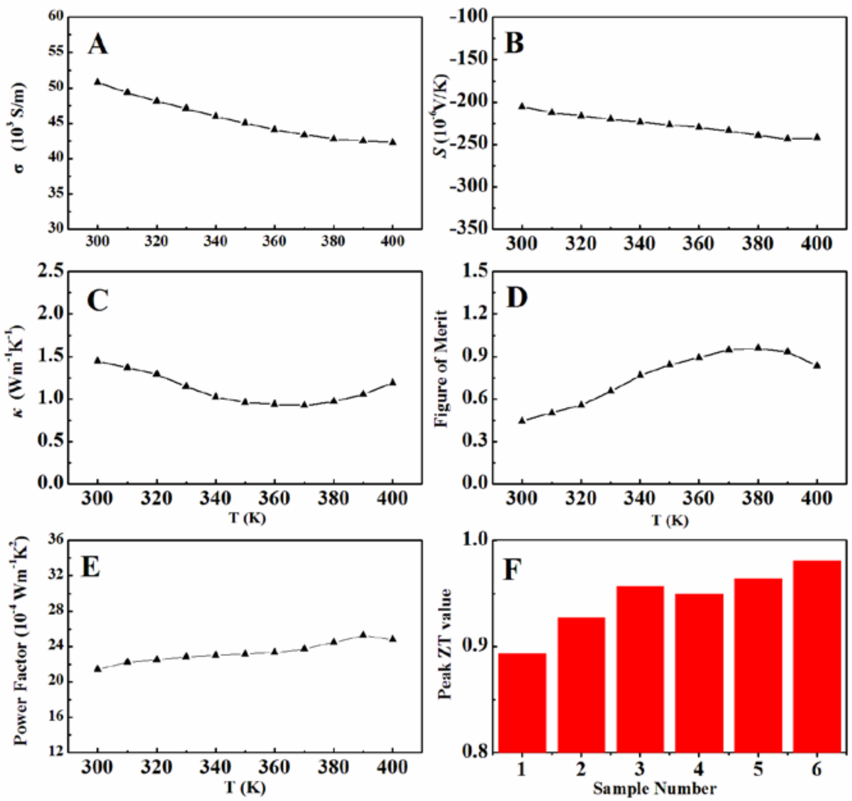

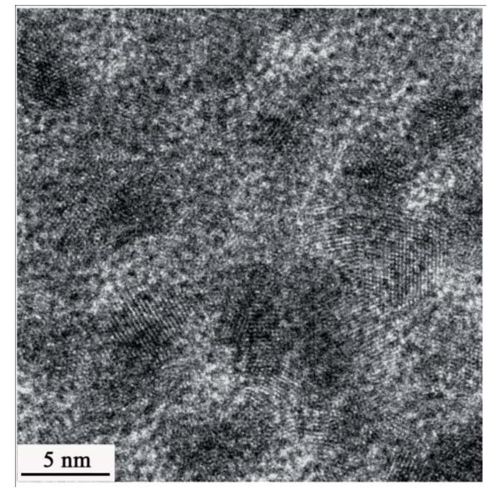

A scalable solution phase method has been established, for the first time to obtain **n-type Bi2Te3 ultrathin nanowires with an average diameter of 8 nm in high yield (up to 93%).** Thermoelectric properties of bulk pellets fabricated by compressing the nanowire powder through spark plasma sintering have been investigated.

The peak ZT value is around 0.96 at 380 K, corresponding to a 13% enhancement compared to that of n-type commercial $Bi_2Te_{2.7}Se_{0.3}$ single crystals (~0.85) and comparable to the best reported result of n-type $Bi_2Te_{2.7}Se_{0.3}$sample (ZT=1.04) fabricated by hot pressing of ball-milled powder.

Zhang, Genqiang; Kirk, Benjamin; Jauregui, Luis A.; Yang, Haoran; Xu, Xianfan; Chen, Yong P.; Wu, Yue* Rational Synthesis of Ultrathin n-type Bi2Te3 Nanowires with Enhanced Thermoelectric Properties. *Nano Letters*, 2012, 12, 56-60.

Nanostructured Thermoelectric Materials

- $SrTiO_3$ Nanowires

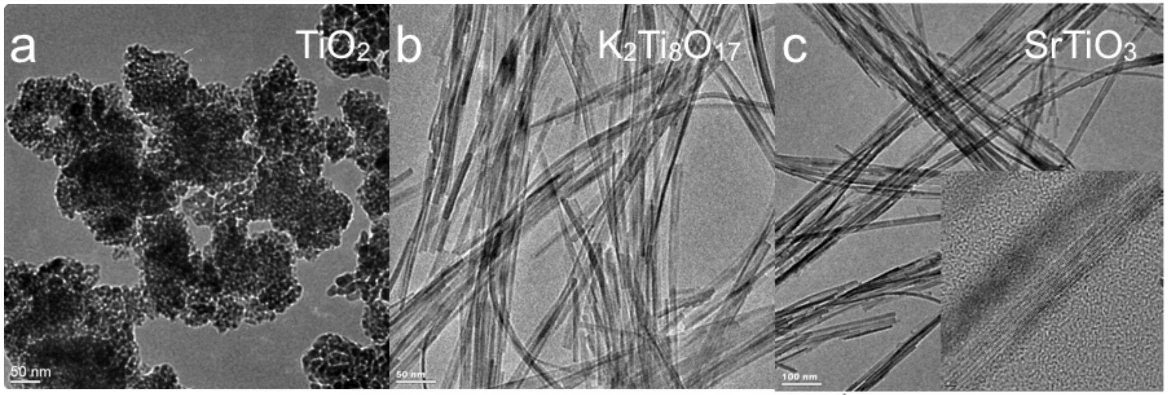

"Self-Templated Synthesis and Thermal Conductivity Investigation for Ultrathin Perovskite Oxide Nanowires", Gautam G. Yadav, Genqiang Zhang, Bo Qiu, Joseph A. Susoreny, XiulinRuan, Yue Wu,* *Nanoscale*, 3, 4078-4081.

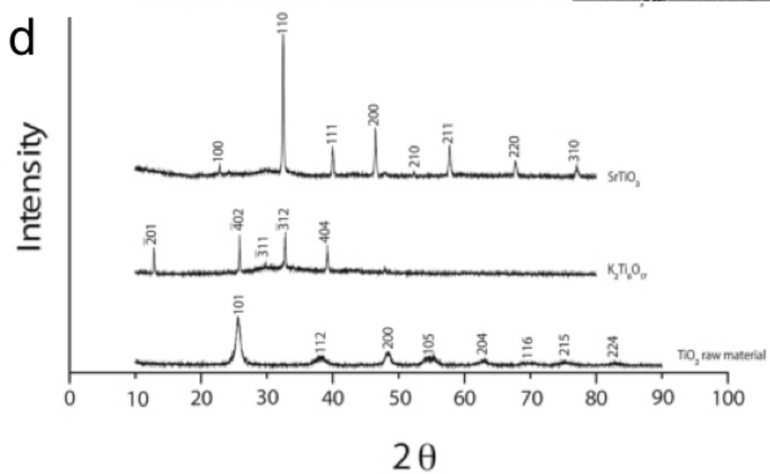

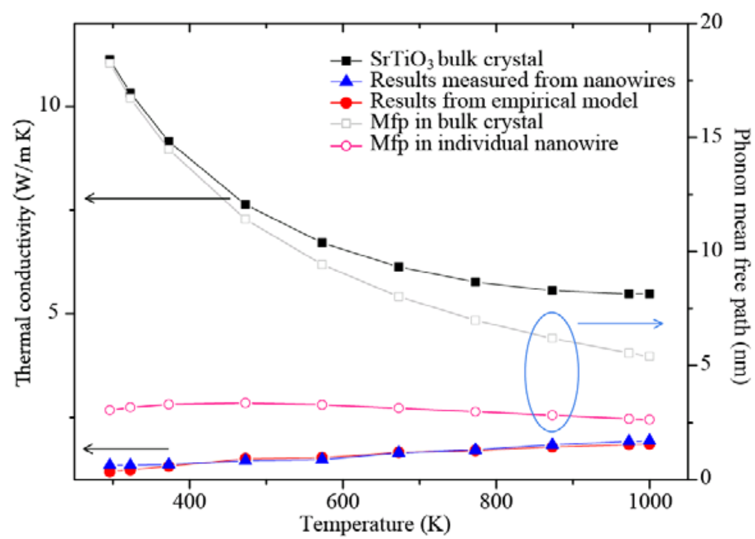

A self-templated synthesis approach to grow ultrathin **SrTiO3 nanowires with an average diameter of 6 nm** in large quantity has been developed. The thermal conductivity of the bulk pellet made by compressing nanowire powder using spark plasma sintering shows a **64% reduction in thermal conductivity at 1000 K**, which agrees well with theoretical modeling.

Thermal Conductivity Reduced 64%

Nanostructured Thermoelectric Materials

- Copper Zinc Tin Sulfide-based TE

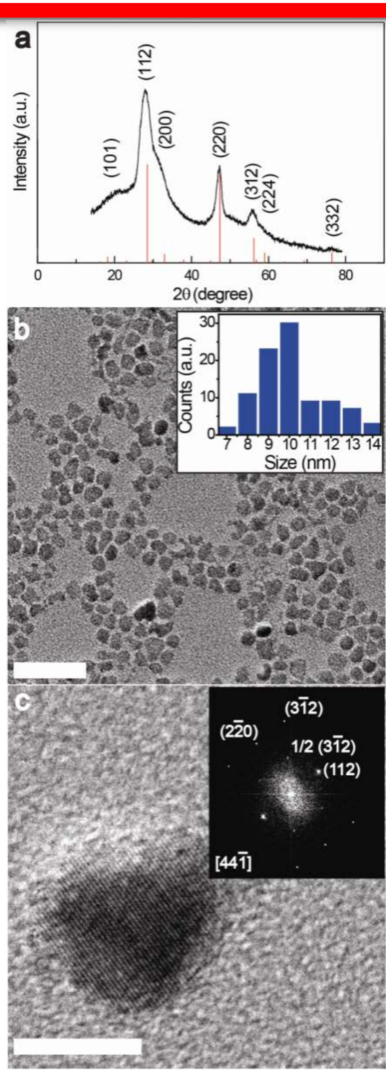

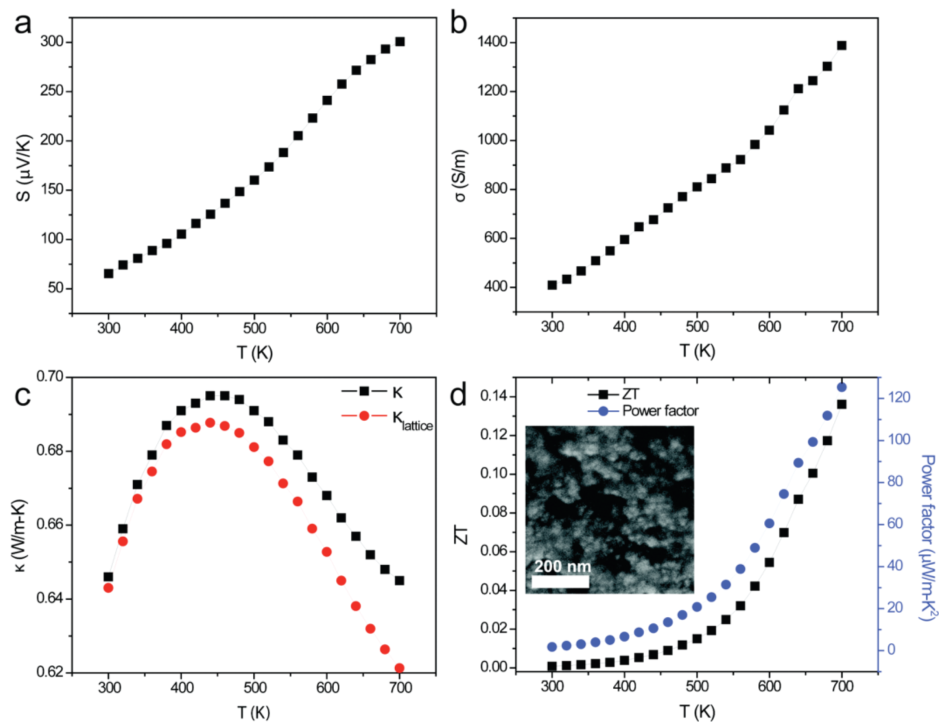

Yang, Haoran; Jauregui, Luis A.; Zhang, Genqiang; Chen, Yong P.; Wu, Yue* Nontoxic and Abundant Copper Zinc Tin Sulfide Nanocrystals for Potential High-Temperature Thermoelectric Energy Harvesting. *Nano Letters*, 2012, 12, 540-545.

The experimental realization of using nontoxic and abundant copper zinc tin sulfide (CZTS) nanocrystals for potential thermoelectric applications. The CZTS nanocrystals can be synthesized in large quantities from solution phase reaction and compressed into robust bulk pellets through spark plasma sintering and hot press while still maintaining nanoscale grain size inside. Electrical and thermal measurements have been performed from 300 to 700 K to understand the electron and phonon transports. Extra copper doping during the nanocrystal synthesis introduces a significant improvement in the performance.

Nanostructured Thermoelectric Materials
- Nitride metal/semiconductor superlattices

Objective: Design nitride metal/semiconductor superlattices with high ZT

−thermionic emission → enhance $S^2\sigma$

−interface phonon scattering → suppress κ

Why ScN? Rocksalt n-type semiconductor compatible with rocksalt metal nitrides (e.g. ZrN, HfN) → superlattice growth

Why (Sc,Mn)N? Fine tune carrier concentration, carrier type, mobility and electrical transport of semiconductor layers

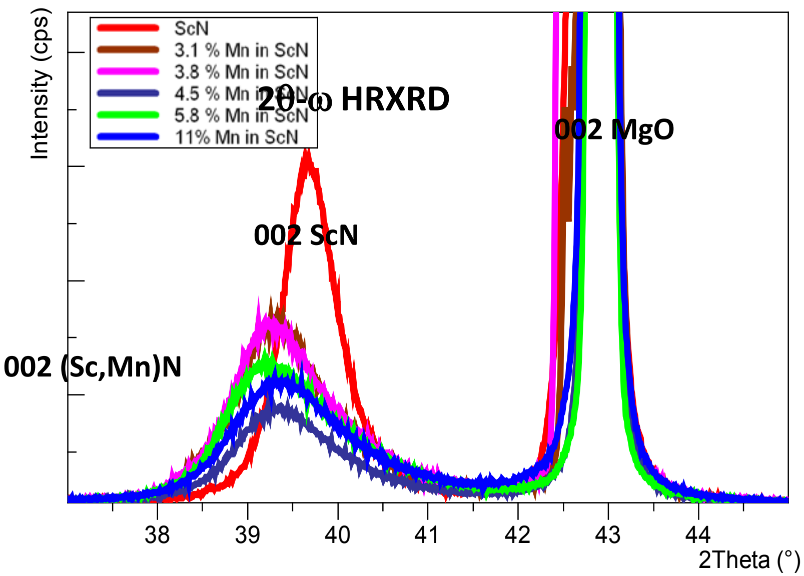

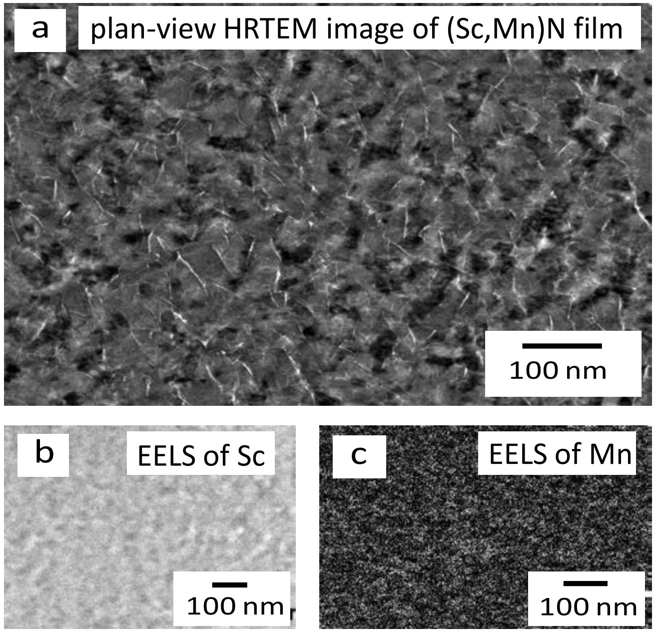

- Mn uniformly distributed
- No secondary phases

Nanostructured Thermoelectric Materials

- (Sc,Mn)N electronic properties

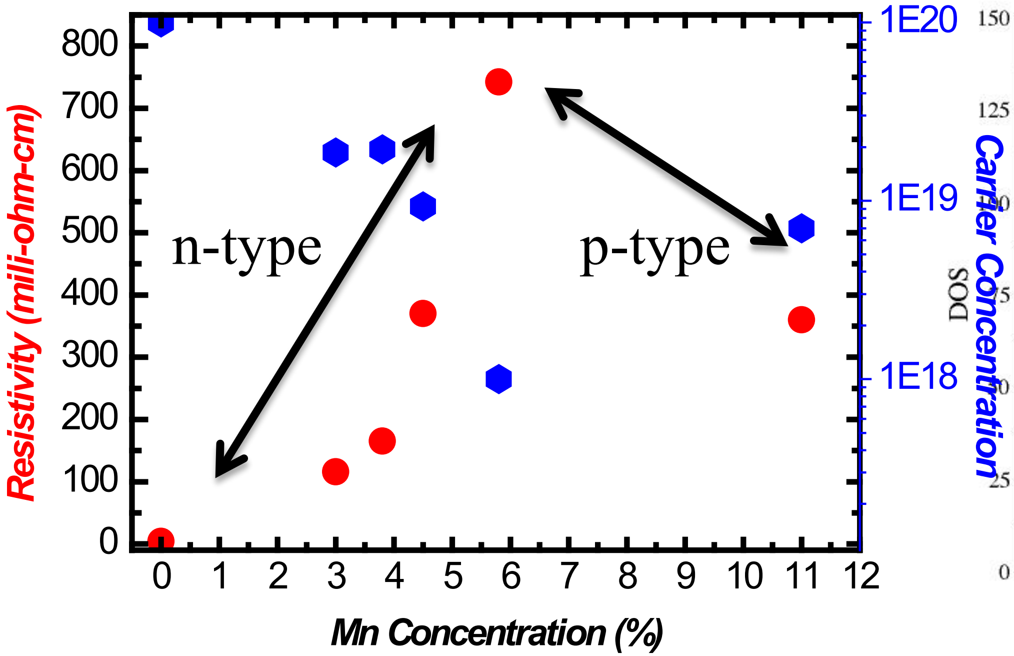

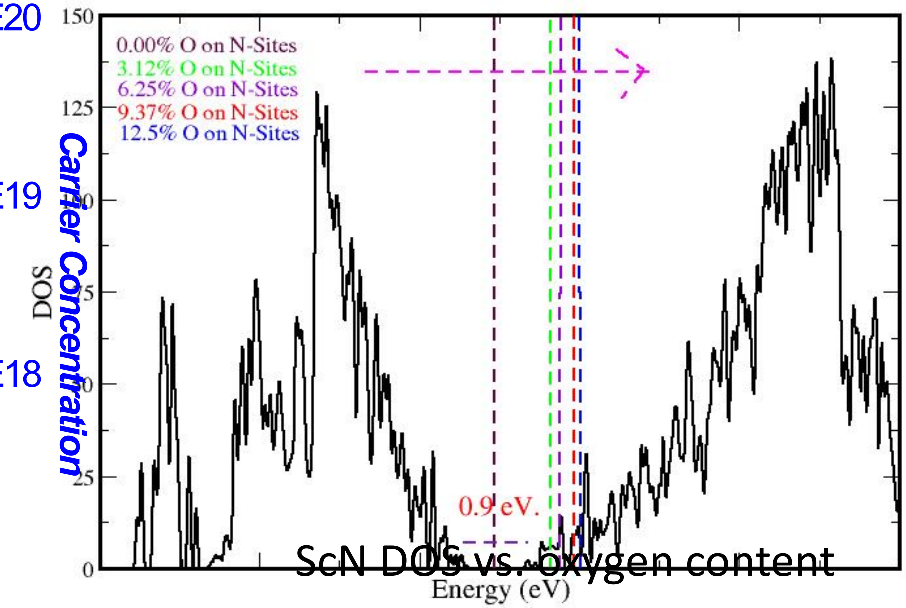

ScN DOS vs. oxygen content

- n-type to p-type transition ≈ 6% Mn

- Fermi level of ScN moves into conduction band with increasing oxygen
- Mn (acceptor) compensates O (donor)

<u>Significant achievement:</u>

•ability to tune the electronic properties of ScN via Mn alloying

Nanostructured Thermoelectric Materials

- (Sc,Mn)N Thermoelectric properties

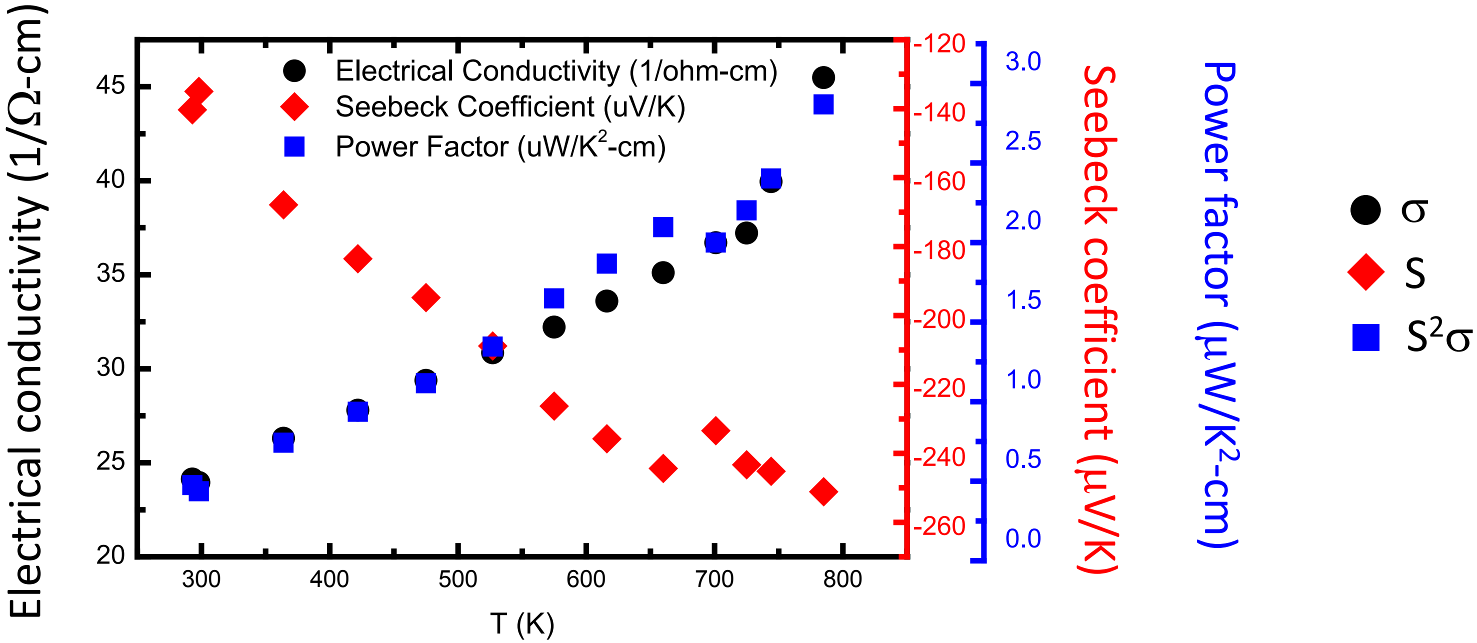

3% Mn doped ScN sample

- Alloying ScN with Mn allows Seebeck coefficient tuning to optimum value (200-250 μV/K)
- Electrical conductivity of (Sc,Mn)N < ScN due to decreased mobility (impurity scattering)

Ongoing Work: Tune growth conditions to optimize $S^2\sigma$

Current Work

(1) TEG system design for specific vehicle requirements and constraints
(2) Systematic ultrafast vibrational spectroscopy studies of filled skutterudites
(3) CNT thermal interface materials optimization and testing
(4) Nanoscale thermoelectric materials characterization